Available online at www.sciencedirect.com
SCIENCE DIRECT®
Journal of Molecular Catalysis A: Chemical 227 (2005) 75–80
JOURNAL OF MOLECULAR CATALYSIS A: CHEMICAL
www.elsevier.com/locate/molcata

Ultrasonic preparation of mesoporous titanium dioxide nanocrystalline photocatalysts and evaluation of photocatalytic activity

Jiaguo Yu[a,*], Minghua Zhou[a,b], Bei Cheng[a], Huogen Yu[a], Xiujian Zhao[a]

[a] *State Key Laboratory of Advanced Technology for Material Synthesis and Processing, Wuhan University of Technology, Wuhan 430070, PR China*
[b] *Staff Room of Chemistry, Yunyang Medical College, Shiyan 442000, Hubei, PR China*

Received 27 August 2004; received in revised form 8 October 2004; accepted 9 October 2004
Available online 21 November 2004

Abstract

Mesoporous titanium dioxide nanocrystalline powders were synthesized by ultrasonic-induced hydrolysis reaction of tetrabutyl titanate ($Ti(OC_4H_9)_4$) in pure water without using any templates or surfactants. The as-prepared samples were characterized with X-ray diffraction (XRD) and N_2 adsorption–desorption measurements. The photocatalytic activity of the samples was evaluated using the probe reaction: the photocatalytic oxidation of mixture of formaldehyde and acetone at room temperature. It was found that the as-prepared products by the ultrasonic method were composed of anatase and brooktie phases. The photocatalytic activity of the samples prepared by ultrasonic method is higher than that of commercial Degussa P25 and the samples prepared by conventional hydrolysis method.

Keywords: TiO_2; Mesoporous; Nanocrystalline; Ultrasonic-induced hydrolysis; Photocatalytic degradation; Formaldehyde; Acetone

1. Introduction

In 1972, Fujishima and Honda discovered the photocatalytic splitting of water on TiO_2 electrodes [1]. This event marked the beginning of a new era in heterogeneous photocatalysis. Since then, the investigation of TiO_2 has become a hot issue. In recent years, in order to solve the increasingly serious problems of environmental pollution, various advanced techniques were applied in the fields of environmental protection. Heterogeneous photocatalysis is a popular technique that has great potential to control aqueous organic contaminates or air pollutants. Among various oxide semiconductor photocatalyst, titanium dioxide has proved to be the most suitable catalysts for widespread environmental application because of its biological and chemical inertness, strong oxidizing power, non-toxicity and long-term stability against photo and chemical corrosion [2–8]. However, the photocatalytic activity of TiO_2 must be further enhanced from the point of view of practical use and commerce [9]. To achieve this purpose, mesoporous TiO_2 has attracted much attention due to its high surface area and large uniform pores.

Various mesoporous materials have been synthesized via conventional approaches using surfactants as templates based on a liquid crystal template mechanism [10]. These methods often require a long time and multiple-step procedures. Sonochemistry has been proven to be an excellent method for the preparation of mesoporous materials [11,12]. It arises from acoustic cavitations, the formation, growth, and implosive collapse of bubbles in a liquid. The collapse of bubbles generates localized hot spots with transient temperatures of about 5000 K, pressure of about 20 MPa, and heating and cooling rates greater than 10^9 K s^{-1} [13,14]. These conditions accelerate the hydrolysis reaction.

In this work, the mesoporous TiO_2 nanocrystalline photocatalysts with bi-phase structure were prepared by sonochemical method without using any templates and surfactants at the room temperature. The as-prepared samples were characterized with X-ray diffraction (XRD) and N_2 adsorption–desorption measurements. The photocatalytic

* Corresponding author. Tel.: +86 27 87883610; fax: +86 27 87883610.
E-mail address: jiaguoyu@yahoo.com (J. Yu).

1381-1169/$ – see front matter © 2004 Elsevier B.V. All rights reserved.
doi:10.1016/j.molcata.2004.10.012

activity of the as-prepared samples was evaluated by the photocatalytic oxidation of the mixture of formaldehyde and acetone in air.

2. Experimental

2.1. Synthesis

Tetrabutyl titanate ($Ti(OC_4H_9)_4$, TBOT) was used as a titanium source. TBOT (8.8 ml) was added dropwise to 40 ml pure water in a 100 ml beaker under irradiation with a high intensity ultrasonic horn (6.3 mm diameter Ti-horn, 20 kHz, and 1200 W/cm^2 at 50% efficiency) (KS-1200: Ningbo Kesheng Ultrasonic Equipment Co. Ltd., Zhejiang, China) for 45 min. The ultrasonic system is 2 s on and 2 s off in air during the whole reaction. After ultrasonic reaction, the precipitate was centrifuged and washed with distilled water. Then the wet gel was dried under an IR lamp and the temperature was below 373 K. The obtained white xerogel powder was labeled as Ti-US373. The xerogel powder was calcined at 573 and 773 K for 2 h, labeled as Ti-US573 and Ti-US773, respectively. As reference experiments, samples were also prepared by conventional hydrolysis method without ultrasonic irradiation, and all other conditions keep the same. The obtained samples at 373, 573 and 773 K were labeled as Ti-CH373, Ti-CH573 and Ti-CH773, respectively.

2.2. Characterization

The X-ray diffraction (XRD) patterns obtained on a diffractometer (type HZG41B-PC) using Cu Kα radiation at a scan rate (2θ) of $0.05^\circ\,s^{-1}$ were used to determine the identity of any phase present and their crystallite size. The accelerating voltage and the applied current were 15 kV and 20 mA, respectively. Titania has three different crystalline phases: rutile, anatase and brookite. Rutile is a thermodynamic stable state while the latter two phases are metastable state. The phase content of a sample can be calculated from the integrated intensities of anatase (1 0 1), rutile (1 1 0) and brookite (1 2 1) peaks. If the sample contains anatase and brookite phases, the mass fraction of brookite can be calculated according to Eq. (1) [15–18].

$$W_B = \frac{2.721A_B}{0.886A_A + 2.721A_B} \quad (1)$$

where A_A and A_B represent the integrated intensities of the anatase (1 0 1) and brookite (1 2 1) peaks, respectively. The average crystallite sizes of anatase and brookite were determined according to the Scherrer equation using the full-width half-maximum data of each phase after correcting the instrumental broading [15–18].

The Brunauer–Emmett–Teller (BET) surface area (S_{BET}) of the samples was analyzed by nitrogen adsorption in an AUTOSORB-1 (Quantachrome Instruments) nitrogen adsorption apparatus. The as-prepared xerogel samples at 373 K were degassed at 353 K, and P25 and the calcined samples were degassed at 453 K prior to nitrogen adsorption measurements. The BET surface area was determined by multipoint BET method using the adsorption data in the relative pressure (P/P_0) range of 0.05–0.3. The desorption isotherm was used to determine the pore size distribution using the Barret–Joyner–Halender (BJH) method with cylindrical pore size [19]. The nitrogen adsorption volume at the relative pressure (P/P_0) of 0.994 was used to determine the pore volume and average pore size.

2.3. Measurement of photocatalytic activity

Formaldehyde and acetone are indoor air pollutants in modern houses, which have been the subject of numerous complaints regarding health disorders, such as nausea, headache, fatigue, dullness and thirst [20,21]. These volatile harmful gases come from plywood, particleboard and adhesives for wall clothes, commonly used in construction and furnishing. In order to improve indoor air quality (IAQ), these volatile organic compounds (VOC) must be eliminated. Therefore, we choose formaldehyde and acetone as model contaminates. Photocatalytic oxidations of formaldehyde and acetone are based on the following reactions [4,5,22]:

$$HCOH + O_2 \rightarrow CO_2 + H_2O \quad (2)$$

$$CH_3COCH_3 + 4O_2 \rightarrow 3CO_2 + 3H_2O \quad (3)$$

The photocatalytic activity experiments on the prepared TiO_2 powders and Degussa P25 (P25) for the oxidations of formaldehyde and acetone in air were performed at ambient temperature using a 15 L photocatalytic reactor. The catalysts were prepared by coating an aqueous suspension of TiO_2 powders onto three dishes with a diameter of about 7.5 cm. The weight of catalysts used for each experiment was kept 0.3 g. The dishes containing catalysts were dried in an oven at 373 K for 2.5 h to evaporate the water and then cooled to room temperature before used. After sample-coated dishes were placed in the reactor, a small amount of formaldehyde and acetone was injected into the reactor with a syringe. The reactor was connected to a $CaCl_2$-containing dryer used for controlling the initial humidity in the reactor. The analysis of formaldehyde, acetone, carbon dioxide, and water vapor concentration in the reactor was conducted on line with a Photoacoustic IR Multigas Monitor (INNOVA Air Tech Instruments Model 1312). The formaldehyde and acetone vapor were allowed to reach adsorption equilibrium with catalysts in the reactor prior to UV light irradiation. The initial concentration of formaldehyde and acetone after adsorption equilibrium were controlled to 250 ± 20 ppm, which remained constant for about 2–3 min until a 15 W 365 nm UV lamp in the reactor was turned on. Integrated UV intensity in the range 310–400 nm striking the coatings was measured with a UV radiometer (Model: UV-A, made in Photoelectric Instrument Factory of Beijing Normal University) was 120 ± 10 μW/cm^2, while the peak wavelength of UV light

was 365 nm. The initial concentration of water vapor was 1.20 ± 0.01 vol.%, and the initial temperature was $25 \pm 1\,^{\circ}C$. Each set of experiment was followed for 50 min.

The photocatalytic activity of the samples can be quantitatively evaluated by comparing the removal efficiency of formaldehyde and acetone (R (%)). R (%) was calculated according to the following equation:

$$R(\%) = \frac{[\text{gas}]_0 - [\text{gas}]_t}{[\text{gas}]_0} \times 100\% \quad (4)$$

where $[\text{gas}]_0$ and $[\text{gas}]_t$ represent the initial equilibrium concentration and reaction concentration of formaldehyde or acetone, respectively.

3. Results and discussions

3.1. XRD study

XRD was used to investigate the phase structures and average crystallite size of the as-prepared TiO_2 powders. Fig. 1(a) shows the XRD patterns of the TiO_2 powder samples prepared by ultrasonic method and calcined at different temperatures. The diffraction peaks of all samples were indexed with the anatase and brooktie phase of TiO_2, which was consistent with our previous work [16–18]. With increasing calcination temperature, the peaks became sharp. This implied that the grain size of all samples became bigger (as shown in Table 1). However, it was noteworthy to note that nanocrystalline TiO_2 formed before heating treatment. This was ascribed to the fact that the implosive collapse of bubbles in a liquid solution could produce extremely high temperature during ultrasonic-induced hydrolysis, which accelerated the reaction of hydrolysis and promoted to the formation of anatase and brooktie phases.

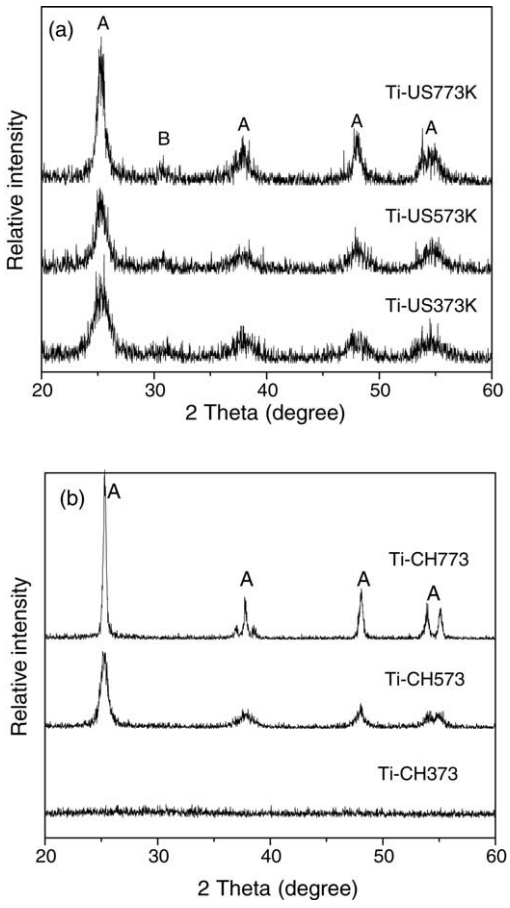

Fig. 1. XRD patterns of Ti-US samples (a) and Ti-CH samples (b) calcined at different temperatures. A: anatase, B: brookite.

Fig. 1(b) shows the XRD patterns of the samples prepared by conventional hydrolysis method. The phase structure of the samples prepared by conventional hydrolysis method was obviously different from that of the samples prepared by ultrasonic-induced hydrolysis method (as shown in Fig. 1(a)). At 373 K, the as-prepared xerogel powder was amorphous. This was probably due to the fact that when alkoxide was hydrolyzed in water without sonication at room temperature, there were a large amount of unhydrolyzed alkyls remained in the xerogel. These alkyls prevented crystallization to anatase so that powders were amorphous by adsorbing on the surfaces of TiO_2 particles [23]. At 573 K, the XRD diffraction peaks of anatase appeared due to crystallization of TiO_2. From 573 to 773 K, the diffraction peak intensities of anatase slightly increased and the width of the (1 0 1) plane diffraction peak of anatase ($2\theta = 25.4$) became narrower. At 773 K, the crystallite size of anatase reached to 56.6 nm (as shown in Table 1). The rapid increase of anatase crystallite size was attributed to the fact that the phase transformation of amorphous to anatase occurred at about 573 K and combustion of residual organic components in xerogel caused the growth of anatase crystallites by providing the heat of phase transformation and combustion.

3.2. BET surface areas and pore distribution

Fig. 2(a) shows the nitrogen adsorption–desorption isotherms of the samples prepared by ultrasonic method. All Ti-US samples showed the isotherms of type IV (BDDT classification) [19]. At high relative pressures from 0.4 to 1.0, the isotherms exhibited hysteresis loops of type H3, indicating that the powders contained mesopores (2–50 nm). With increasing calcination temperature, the hysteresis loops shifted to the region of higher relative pressure and the areas of the hysteresis loops gradually became small.

Fig. 2(b) shows the nitrogen adsorption–desorption isotherms of the samples prepared by conventional hydrolysis method. It could be seen that the adsorption–desorption isotherms of the samples prepared by conventional hydrolysis method were obviously different from those of the samples prepared by ultrasonic-induced hydrolysis method (as shown in Fig. 2(a)). The isotherm of Ti-CH373 was a combination of types I and IV (BDDT classification) with two very distinct regions: at low relative pressure, the isotherm exhibited high adsorption, indicating that the powder contained micropores

Table 1
Effects of calcination temperature and preparation method on physical properties of TiO_2 powder photocatalyst

Sample	Phase content[a]	Crystalline size (nm)[b]	Surface area (m^2/g)[c]	Pore volume (ml/g)[d]	Average pore size (nm)[d]
Ti-US373	A (75%) + B (25%)	5.3	264.5	0.285	4.3
Ti-US573	A (81%) + B (19%)	6.2	202.0	0.286	5.7
Ti-US773	A (63%) + B (37%)	10.9	97.3	0.222	9.1
Ti-CH373	Am	–	460.1	0.280	2.4
Ti-CH573	A	14.2	84.9	0.112	5.3
Ti-CH773	A	56.6	5.9	0.001	6.0
P25	A (80%) + R (20%)	30.0	63.0	0.060	3.8

[a] A, B, R and Am denote anatase, brookite, rutile and amorphous, respectively.
[b] Average crystalline size of TiO_2 was determined by XRD using Scherrer equation.
[c] The BET surface area was determined by multipoint BET method using the adsorption data in the relative pressure (P/P_0) range 0.05–0.3.
[d] Pore volume and average pore size were determined by nitrogen adsorption volume at the relative pressure of 0.994.

(type I). However, at high relative pressure between 0.5 and 1.0, the curve exhibited a very small hysteresis loop, indicating the presence of mesopores (type IV). The isotherm of the Ti-CH573 exhibited a hysteresis loop at relative pressure between 0.5 and 0.8, indicating that the presence of mesopore. While the Ti-CH773 sample almost had no hysteresis loop, indicating that all the pores collapsed during calcination and the total pore volume was very small.

Fig. 2(c) shows the pore size distribution curves of the samples prepared by ultrasonic method. It could be seen that the diameter range of pores were located at from 2.0 to 16.0 nm and the average diameter of pores did not exceed 10 nm (as shown in Table 1). The formation of mesoporous structure in the samples was attributed to the aggregation of TiO_2 particles [22,24]. With increasing calcination temperature, the average pore size increased from 4.3 to 9.1 nm. There were two factors resulting in the increase of pore size. One was that the smaller pores endured much greater stress than the bigger pores, so the small pores collapsed firstly during calcination. The other was that the bigger crystallites aggregation could form bigger pores. Therefore, with increasing calcination temperature, the pores became bigger while pore volume became smaller.

It could also be seen from Fig. 2(d) that the pore size distribution curves of the samples prepared by conventional hydrolysis method at different temperature were very different. At 373 K, the Ti-CH373 sample had a wide pore size distribution from micropore to mesopore. With increasing calcination temperature, at 573 K, the Ti-CH573 sample had a typical mesoporous pore distribution. However, at 773 K, the pore size distribution curve turned into a line, indicating the disappearance of pores.

Table 1 shows the effects of preparation method and calcination temperature on the physical properties of the as-prepared samples. It could be seen from Table 1 that the Ti-US373 sample prepared by ultrasonic method showed a

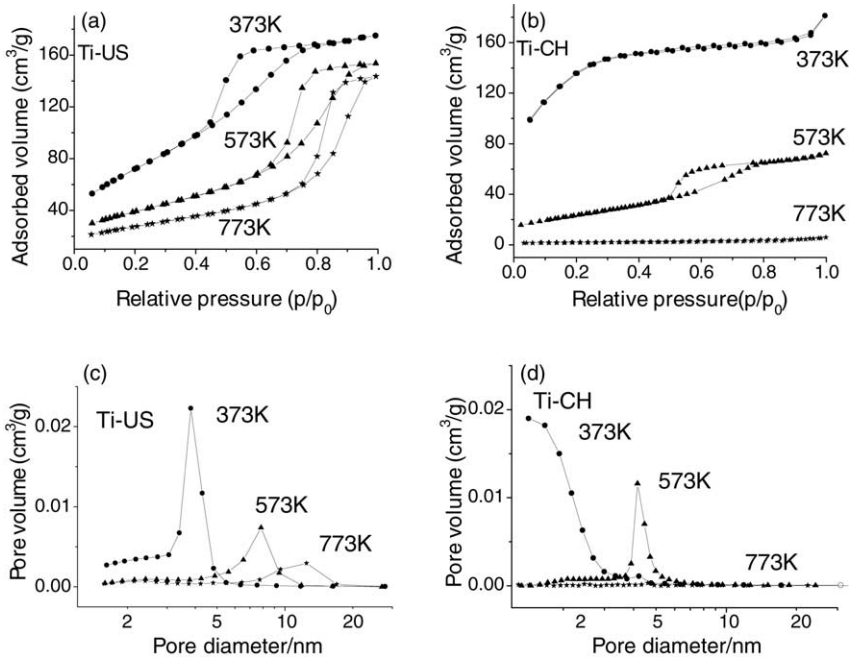

Fig. 2. Adsorption–desorption isotherms (a and b) and pore size distribution (c and d) of Ti-US samples (a and c) and Ti-CH samples (b and d).

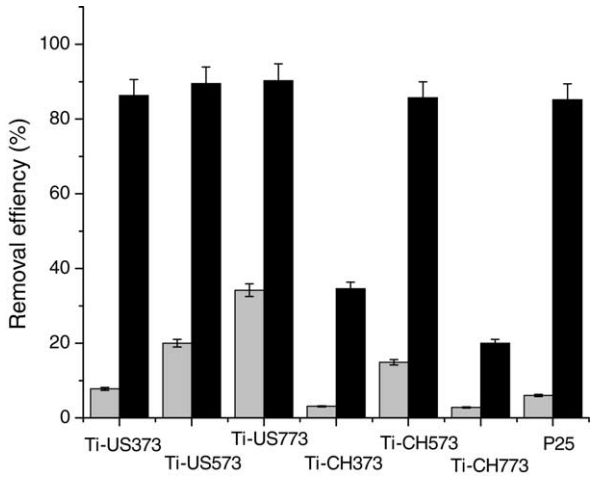

Fig. 3. The removal efficiency of formaldehyde and acetone: dark gray is the removal efficiency of formaldehyde and light gray is the removal efficiency of acetone.

large specific surface area and pore volume, and its values reached 264.5 m^2/g and 0.285 cm^3/g, respectively. With increasing calcination temperature, the specific surface areas and pore volumes steadily decreased due to the growth of TiO_2 crystallites. At 773 K, the specific surface area and pore volume of the Ti-US773 sample decreased to 97.3 m^2/g and 0.222 cm^3/g, respectively. On the other hand, for the Ti-CH samples prepared by conventional hydrolysis method, their specific surface area, pore volume and average pore size drastically decreased with increasing calcination temperature. At 373 K, the Ti-CH373 sample showed a very large S_{BET} value of 460.1 m^2/g. This was probably due to the fact that its phase structure appeared amorphous. From 373 to 573 K, the phase transformation from amorphous to anatase occurred. At 573 K, the average crystallite size of anatase was 14.2 nm. At 773 K, the average crystallite size of anatase increased to 56.6 nm. Why the calcination had a greater effect on the crystallite size of the Ti-CH samples than the Ti-US samples? This was assigned to the fact that the phase transformation of amorphous to anatase and combustion of residual organic components in the Ti-CH samples promoted the crystallization and the growth of crystallite size.

3.3. Photocatalytic activity

Fig. 3 shows that the comparison of photocatalytic activity of the as-prepared samples by the ultrasonic-induced hydrolysis and conventional hydrolysis method and P25. It could be seen from Fig. 3 that the removal efficiency of formaldehyde (R (%)) was obviously higher than that of acetone for all catalysts. This might be due to the fact that acetone contained more carbon atoms and had greater space hindrance than formaldehyde. Fig. 3 also showed that the removal efficiencies of formaldehyde for all the catalysts were similar and had no distinct difference. Hence, it could be inferred that acetone gas as model containment was more reasonable.

Fig. 3 shows that the samples prepared by ultrasonic method had better activities than the samples prepared by conventional hydrolysis method. This was attributed to the fact that the samples prepared by ultrasonic method had a bi-phase structure [9,12]. At 373 K, the Ti-US373 sample showed decent photocatalytic activity and the removal efficiency of formaldehyde and acetone were 86.0% and 8.0%, respectively. For the removal of acetone, the photocatalytic activities of Ti-US373, Ti-US573 and Ti-US773 samples greatly exceeded that of Degussa P25 (the removal efficiency of formaldehyde and acetone are 85.0% and 5.0%, respectively.). This might be attributed to the fact that the former had a larger specific surface area, smaller crystallite size, etc. For the Ti-US samples, with increasing calcination temperature, the photocatalytic activities of Ti-US373, Ti-US573 and Ti-US773 samples steadily increased. This was probably due to the enhancement of crystallization [9,12,25]. While for the Ti-CH373 sample, it showed a very low photocatalytic activity and the removal efficiencies of formaldehyde and acetone were 35.0% and 3.0%, respectively. For all Ti-CH samples, only the photocatalytic activity of Ti-CH573 approached to that of Degussa P25. This might be ascribed to the following facts that, at low temperature (373 K), the Ti-CH373 sample prepared by conventional hydrolysis method was amorphous, while the Ti-US373 sample prepared by ultrasonic method was nanocrystallite. Therefore, the Ti-CH373 sample showed a low photocatalytic activity. At high temperature (773 K), the S_{BET} and total pore volume of the Ti-CH773 sample were much smaller than those of the Ti-US773 samples and P25. Therefore, the photocatalytic activity of Ti-US773 sample significantly decreased.

4. Conclusion

1. Highly photocatalytic active mesoporous nanocrystalline TiO_2 powder photocatalyst could be prepared using a sonochemical technique without using any templates or surfactants at low temperature. The sonication promoted the hydrolysis of TBOT, crystallization of TiO_2 and formation of mesopore.
2. All the samples prepared by ultrasonic method showed better photocatalytic activities than Degussa P25 and the samples prepared by conventional hydrolysis method. This may be ascribed to the facts that the samples prepared by ultrasonic method have high specific surface area, small particle size and bi-phase structures.
3. The formaldehyde is more easily photocatalytic decomposed than acetone due to its less carbon atoms and smaller space hindrance.

Acknowledgements

This work was partially supported by the National Natural Science Foundation of China (50272049, 20473059). This

work was also financially supported by the Excellent Young Teachers Program of MOE of China and Project-Sponsored by SRF for ROCS of SEM of China.

References

[1] K. Honda, A. Fujishima, Nature 238 (1972) 37.
[2] H. Tada, M. Yamamoto, S. Ito, Langmuir 15 (1999) 3699.
[3] M.A. Fox, M.T. Dulay, Chem. Rev. 93 (1993) 341.
[4] M.R. Hoffmann, S.T. Martin, W. Choi, D.W. Bahnemann, Chem. Rev. 95 (1995) 69.
[5] A. Fujishima, T.N. Rao, D.A. Tryk, J. Photochem. Photobiol. C: Photochem. Rev. 1 (2000) 1.
[6] J.G. Yu, H.G. Yu, B. Cheng, X.J. Zhao, J.C. Yu, W.K. Ho, J. Phys. Chem. B 107 (2003) 13871.
[7] J.C. Zhao, T.X. Wu, K.Q. Wu, K. Oikawa, H. Hidaka, N. Serpone, Environ. Sci. Technol. 32 (1998) 2394.
[8] Y.M. Xu, C.H. Langford, Langmuir 17 (2001) 897.
[9] J.G. Yu, J.G. Yu, W.K. Ho, L.Z. Zhang, Chem. Commun. (2001) 1942.
[10] N. Perkas, O. Palchik, I. Brukental, I. Nowik, Y. Gofer, Y. Koltypin, A. Gedanken, J. Phys. Chem. B 107 (2003) 8772.
[11] J.G. Yu, J.C. Yu, W.K. Ho, M.K.P. Leung, B. Cheng, G.K. Zhang, X.J. Zhao, Appl. Catal. A 255 (2003) 309.
[12] J.C. Yu, J.G. Yu, W.K. Ho, Z.T. Jiang, L.Z. Zhang, Chem. Mater. 14 (2002) 3808.
[13] A. Gedanken, X. Tang, Y. Wang, N. Perkas, Y. Koltypin, N. Perkas, Y. Koltypin, M.V. Landau, L. Vradman, M. Herskowitz, Chem. Eur. J. 2 (2001) 4547.
[14] K.S. Suslick, S.B. Choe, A.A. Cichowlas, M.W. Grinstaff, Nature 353 (1991) 414.
[15] H. Zhang, J. Banfield, J. Phys. Chem. B 104 (2000) 3481.
[16] J.G. Yu, J.C. Yu, B. Cheng, S.K. Hark, K. Iu, J. Solid State Chem. 174 (2003) 372.
[17] J.G. Yu, J.C. Yu, B. Cheng, X.J. Zhao, Sci. China B 46 (2003) 449.
[18] J.G. Yu, J.C. Yu, Chin. J. Chem. 21 (2003) 994.
[19] K.S.W. Sing, D.H. Everett, R.A.W. Haul, L. Moscou, R.A. Pierotti, J. Rouquerol, T. Siemieniewska, Pure Appl. Chem. 57 (1985) 603.
[20] M.E. Zorn, D.T. Tompkins, W.A. Zeltner, M.A. Anderson, Appl. Catal. B 23 (1999) 1.
[21] Y. Sekine, Atmos. Environ. 36 (2002) 5543.
[22] J.G. Yu, J.C. Yu, M.K.P. Leung, W.K. Ho, B. Cheng, X.J. Zhao, J.C. Zhao, J. Catal. 217 (2003) 69.
[23] S. Ito, S. Inoue, H. Kawada, H. Hara, M. Iwasaki, H. Tada, J. Colloid Interf. Sci. 216 (1999) 59.
[24] W. Huang, X. Tang, Y. Wang, Y. Koltypin, A. Gedanken, Chem. Commun. (2000) 1415.
[25] F.B. Li, X.Z. Li, M.F. Hou, Appl. Catal. B 48 (2004) 185.